Journal of Radiotherapy in Practice

cambridge.org/jrp

Optimizing MRI pulse sequence for displaying gold markers in radiation therapy simulation of patients with prostate cancer

Fariba Bagheri[1], Fariborz Faeghi[1], Banafsheh Baniasadipour[1], Mohsen Bakhshandeh[1], Samira Azghandi[2] and Farzane Hendudari[3]

[1]Department of Radiology Technology, Allied Medical Faculty, Shahid Beheshti University of Medical Sciences, Tehran, Iran; [2]Shohadaye Tajrish Hospital, Tehran, Iran and [3]Ayatollah-Khansari hospital, Arak University of Medical Sciences, Arak, Iran

Original Article

Cite this article: Bagheri F, Faeghi F, Baniasadipour B, Bakhshandeh M, Azghandi S, and Hendudari F. (2024) Optimizing MRI pulse sequence for displaying gold markers in radiation therapy simulation of patients with prostate cancer. *Journal of Radiotherapy in Practice*. **23**(e15), 1–6. doi: 10.1017/S1460396924000116

Received: 20 August 2023
Revised: 29 November 2023
Accepted: 7 April 2024

Keywords:
CT; gold marker; prostate cancer; 3D GRE T_2*

Corresponding author:
Mohsen Bakhshandeh;
Email: mbakhshandeh@sbmu.ac.ir

Abstract

Background: Magnetic resonance localization of gold markers for radiotherapy is critical for the treatment planning of prostatic cancer. This study sought to enhance the visualization of gold markers by applying the three-dimensional gradient echo (3D GRE) T_2* sequence and comparing it with CT scan.
Methods: 29 Patients who underwent both a 3D GRE T_2* sequence and a CT were evaluated by an oncologist and radiologist. The SNR, CNR and prostate volume were calculated.
Result: The depiction of gold markers using 3D GRE T_2* exhibited an enhanced quality in comparison to CT ($p < 0{\cdot}05$). Prostate SNR, fat SNR, muscle SNR and Osteon SNR were found to be elevated in 3D GRE T_2*, as opposed to the CT ($p < 0{\cdot}05$). The comparison of the average prostate volume revealed a significant difference between the mean measurements (sig = 0, $p < 0{\cdot}05$). The prostate Volume in 3D GRE T_2* 29·03% smaller in magnitude when compared to the CT, thus bringing it into closer alignment with its authentic dimensions.
Conclusion: The comparison between the MRI and the CT demonstrated that 3D GRE T_2* is an exceptional tool for visualizing gold markers in the realm of prostate cancer radiotherapy planning. It has the potential to minimize collateral damage to healthy cells while enhancing the precision of cancer cell targeting.

Introduction

Prostate cancer, in the year 2020, exhibited itself as the fourth most prevalent form of cancer, as evidenced by the 1,414,259 newly identified cases, as well as 375,304 deaths.[1] Treatment options for prostate cancer mainly depend on the stage and progression of the cancer as well as the occurrence of biochemical failure. When prostate cancer has progressed locally (T3-T4), the disease can be treated through the utilization of radiotherapy in conjunction with androgen deprivation therapy or through the implementation of surgery in conjunction with adjuvant radiotherapy.[2]

External beam radiation therapy (EBRT) is a common treatment for localized prostate cancer. In EBRT, accurate registration and mapping of the prostate contour are important to ensure precise dose delivery to the target area while minimizing radiation exposure to surrounding healthy tissues and organs. Several methods and technologies are employed to achieve accurate prostate registration and mapping in EBRT. In a traditional computed tomography (CT)-based EBRT workflow, the prostate and other organs at risk (rectum, bladder and bones) are manually contoured on a patient's planning CT scan. This CT scan provides tissue electron densities for dose calculation and enables the generation of digitally reconstructed radiographs (DRRs) for patient set-up verification before each treatment fraction. However, The prostate has low tissue contrast,[3,4] and magnetic resonance imaging (MRI) offers better visualization of soft tissues like the prostate. Therefore, MRI is often fused with the planning CT to improve the accuracy of prostate contouring.

Prostate cancer patients who were scheduled to receive EBRT are commonly implanted with fiducial markers to verify treatment position. Gold fiducial markers have been shown to facilitate landmark-based alignment of MRI to the planning CT image.[5] Currently, these markers are identified using CT imaging, while soft tissues such as the prostate and ORAs such as the bladder and rectum are delineated on MRI, requiring registration of MRI to CT. MRI, characterized by its superior soft tissue contrast resolution, excels in providing detailed depictions of various soft tissue components. However, the registration procedure is prone to errors, which can propagate throughout the entire treatment process.[3,4] The mentioned errors pertain to physiological motion and geometric distortion. Geometric distortion may be attributed to either patient factors or hardware issues, and any such distortion has the potential

© The Author(s), 2024. Published by Cambridge University Press. This is an Open Access article, distributed under the terms of the Creative Commons Attribution licence (http://creativecommons.org/licenses/by/4.0/), which permits unrestricted re-use, distribution and reproduction, provided the original article is properly cited.

to result in registration errors and uncertainties in radiotherapy target localization. The standard geometric distortion area is specified to be less than 2 mm.[6] Although the area of concern in prostate MRI is typically a small distance around the MR isocenter, complete mitigation of geometric distortion may not be achievable, and registration errors are likely. Additionally, it is widely accepted that the registration of MR and CT datasets is unambiguous. However, a multicenter trial utilizing a single head CT-MR test dataset reported an uncertainty of 2 mm.[4]

The introduction of an MR-only workflow is a potential approach to avoiding the need for CT scans in the treatment planning process for prostate cancer. However, successfully implementing an MR-only workflow to reach optimal treatment efficiency requires accurately identifying markers on MRI scans.[7]

The most commonly used markers are made of gold, usually presenting as a local signal void on MR images. Most studies have been performed on optimizing a method for the adaptation of CT and MRI images for a treatment design, and only a few studies have addressed the application of a sequence for a better representation of the gold marker. Most studies utilized the gradient echo (GRE) T2* sequence for marker depiction, leveraging its sensitivity to T2* decay through the susceptibility effect to achieve better marker depiction.[2] GRE T_2* has been suggested as the best sequence for the depiction of gold markers, but the sequence specification varied among different studies.[7,8] Therefore, we designed an optimal MRI sequence (three-dimensional (3D) GRE T2*) and showed the ability of 3D GRE T_2* sequence to depict gold markers and compared it with CT in patients with prostate carcinoma undergoing radiotherapy treatment planning.

Materials and Methods

The study included a total of 29 patients with prostate cancer who were scheduled to undergo EBRT between October 2016 and June 2017. Informed consent was obtained from all participants involved in the study, and the confidentiality of patient data was strictly maintained.

An average of three gold fiducial markers were implanted per patient.[9] Gold seeds employed in prostate RT are approximately 5 mm in diameter, although larger cylindrical markers are also available.[4] The fiducial gold markers utilized in our study were imported from Primed, a German company. These markers have a cylindrical shape with dimensions of $1 \times 0{\cdot}5$ cm (10×5 mm).

Patients underwent both MRI and CT scan, and the images were utilized for radiotherapy planning purposes. The MRI protocol was 3D GRE T_2*, and the specific parameters of the protocol are outlined in Table 1. The CT scans were obtained using a 16-slice CT scanner (Siemens) with slice thickness of 3 mm. For patients undergoing intensity-modulated radiation therapy, the placement of fiducial markers was required to enhance the co-registration of MR image with CT image treatment planning. Gold seeds were placed under transrectal ultrasound guidance.[10] Subsequently, the overall mean values and standard deviations (SDs), along with random and systematic errors, were calculated.

3D GRE T_2* sequence

Using a single echo per line of K-space in MRI results in acquiring a conventional spoiled GRE sequence, leading to reduced signal to noise ratio (SNR) and necessitating a narrower receiver bandwidth (BW).The T2* decay of transverse magnetization distorts the GRE by decreasing resolution in the frequency direction and inducing geometric distortion. The BW receiver was augmented, theoretically increasing spatial resolution. Likewise, a long time of echo (TE) can be used to increase the magnitude of the susceptibility effect while reducing geometric distortion. In this research, we used small pixel sizes to increase image resolution, as well as 3D imaging to enhance SNR.[2] The details of T2* GRE-3D sequence are presented in Table 2.

Visual and statistical analyses

One radiologist and one oncologist reviewed cases, and readers evaluated three parameters: (i) overall image quality, (ii) depiction of /fiducials (magnitude of signal void) and (iii) image sharpness (degree of geometric distortion and blur). Each sequence was scored on a 5-point scale with : 1 = poor, 2 = suboptimal, 3 = adequate, 4 = above average and 5 = excellent. This scoring scale was adopted from previous studies.[2]

Statistical analysis was performed using IBM SPSS version 24 with Freedman's method, and a p value of $< 0{\cdot}05$ was considered as statistically significant.

Quantitative analysis

Quantitative analysis was conducted on three indicators – contrast to noise ratio (CNR), SNR and prostate volume – in CT and MRI images to compare the sequences. The primary stages of the quantitative analysis were conducted using SINGO on the MRI device. The SNR index was marked by inserting region of interest (ROI) and measuring the average signal strength at three anatomical points of the symphysis pubis bones and the tip of both femurs (center of the bone), three ROIs on the pelvic muscles and lipid tissue on both sides of the prostate (Figure 1) and one ROI outside of the anatomical range on the free space to calculate the standard deviation of the free space (Figure 1). The dimensions of the ROI and the intended section were considered constant in all sequences. To calculate the CNR, we subtracted the mean signal intensity of two areas from the standard deviation of the free space using following equation:

SNR = SI/N
N = Standard deviation air
CNRPO = SIP – SIO/N
CNR PM = SIP – SI M/N
CNR PF = SI P – SI F/N
CNROM = SI O – SI M/N
CNR OF = SI O – SI F/N
CNR FM = SI F – SI M/N
P = Prostate
O = Osteon
F = Fat
M = Muscle
N = SD (air)

To calculate the volume, we initially assessed the sequences wherein the prostate was identified in MRI images, comparing them with the corresponding sections in CT scan images. Then, we obtained the area of all sections separately using SINGO software (software environment at the Siemens MRI workstation) and circled the prostate region, and the area of the cross section was obtained. The total volume of the prostate was calculated by multiplying the area of each prostate section by its thickness and summing the volumes of all sections. In this study, MRI and CT images had a thickness of 3 mm. Earlier studies have suggested that the prostate volume is 30% smaller in MRI images and closer to its real size.[4]

https://doi.org/10.1017/S1460396924000116 Published online by Cambridge University Press

Table 1. Parameters of optimized 3D GRE T_2* sequence

Sequence	Plan	TR (ms)	TE (ms)	Matrix size	Flip angle	FOV (mm)	Slice thickness (mm)	Dimension	Scan time	Number of slices
T2* GRE-3D	Axial	70	18	512 × 448	30	400–430	3	3D	8 min	30

Table 2. Parameters of all MRI sequences

Sequence	Plan	TR(ms)	TE(ms)	Matrix size	Flip angle	FOV (mm)	Slice thickness (mm)	Dimension
T2* GRE-3D	Axial	70	18	512 × 448	30	400–430	3	3D

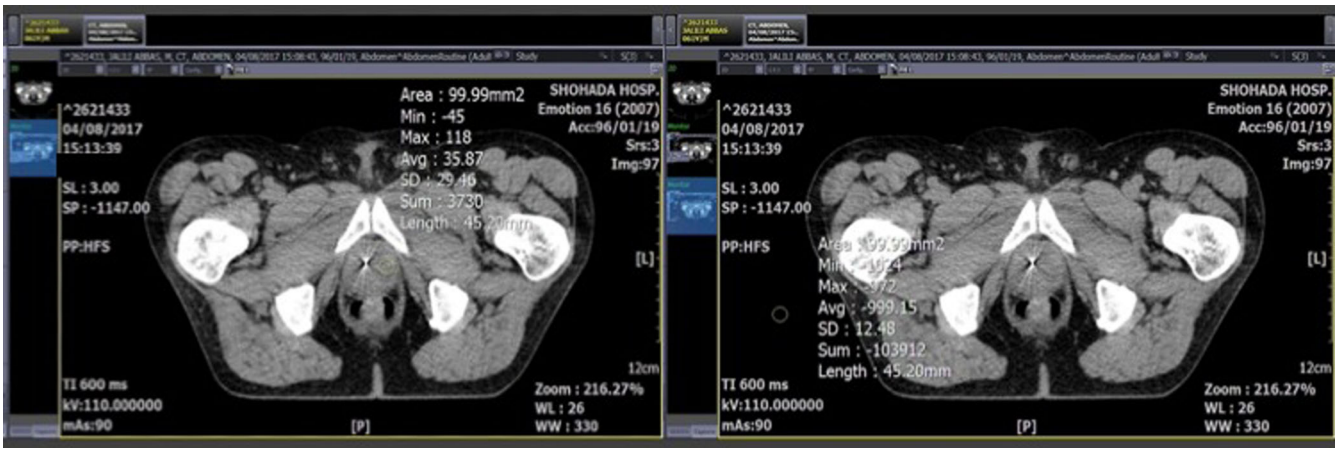

Figure 1. ROI area determination in prostate tissue on CT scan image and the location of ROI on background for calculating of standard deviation.

SNR, CNR and prostate volume were calculated per patient using the SINGO software on the MRI scanner. Statistical analysis, including paired T-test, was conducted using IBM SPSS version 24. A p-value of $< 0{\cdot}05$ was considered statistically significant.

Results

The mean age of patients included in this study was $71{\cdot}37 \pm 7{\cdot}72$ years. According to the 5-point scale which we mentioned before, the oncologist determined that all 29 patients had an adequate depiction of the gold marker in the CT scan. However, according to the radiologist's assessment, 24 patients had suboptimal depiction of the gold markers, while the remaining five had the adequate depiction of the markers.

In term of 3D GRE T2*, the oncologist determined that 17 patients had excellent, nine had above average, one had adequate, one had suboptimal and one had poor depiction of gold markers. While radiologists determined that 16 patients had excellent, 10 had above average, one had adequate and two had suboptimal depiction of gold markers. All of these numbers are written in Table 3.

The depiction of gold markers using 3D GRE T2* imaging was found to be significantly better when compared to CT scan ($p < 0{\cdot}05$). Moreover, prostate SNR, fat SNR, muscle SNR and osteon SNR in 3D GRE T2* images were significantly higher than CT scan ($p < 0{\cdot}05$). We also found that there was a significant difference between SNR in all of the tissues in MRI compared to CT scan (Figure 2).

The results of the comparison of mean prostate volume showed a significant difference between measured numbers ($p < 0{\cdot}05$). In addition, the calculated prostate volume in CT was 29·03% higher than the calculated volume in 3D GRE T2* images, thus the utilization of MRI could show the prostate volume smaller, this finding is also consistent with the previous studies (Figure 3).[4]

This advantage makes it possible to hurt less healthy cells in radiotherapy and focus radiation on cancer cells. Furthermore, 3D GRE T2* showed a higher contrast of all tissues compared to CT scan, and this difference was statistically significant ($p < 0{\cdot}05$) (Figure 4).

This study demonstrated that 3D GRE T2* gave a better picture of implanted fiducial markers (with the highest percentage of susceptibility) and better total image quality and image sharpness in comparison to CT. 3D GRE T2* accurately showed that the implanted seed can be detected within the area of the signal void.

With 3D, T2* weighting was provided by the GRE magnetic susceptibility, which enhances the contrast between the dark seeds and relatively bright pelvic systems. Heightened signal intensity was an added advantage in slow flowing-pelvic veins with T2* weighting because these structures could be readily distinguished from displaced seeds (Figures 5).

Discussion

The alignment between CT and MRI images is essential in ensuring the accuracy of radiotherapy treatment for patients diagnosed with prostate cancer. However, inherent differences between these imaging modalities often lead to errors and challenges during their adaptation. If the gold markers implanted in the prostate were clearly discernible in the MRI scans, only these images could be

https://doi.org/10.1017/S1460396924000116 Published online by Cambridge University Press

Table 3. Result of quality assessment by oncologist and radiologist

Quality assessment levels	Radiologist assessment	Oncologist assessment
Excellent	16	17
Above average	10	9
Adequate	1	1
Suboptimal	2	1
Poor	0	1

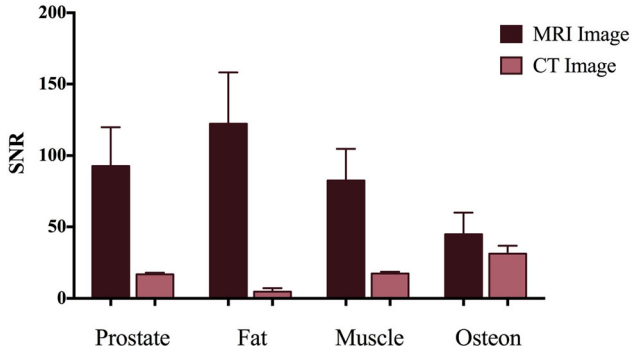

Figure 2. Comparison of different tissues SNR (signal to noise ratio) in CT (computed tomography) and MRI (magnetic resonance imaging), (3D GRE T2*).

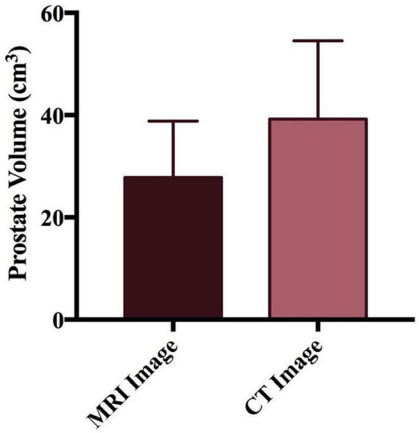

Figure 3. Comparison of prostate volume in CT (computed tomography) and MRI (magnetic resonance imaging), (3D GRE T2*).

utilized for the purpose of designing the radiotherapy treatment. However, it is important to note that these gold markers are not sufficiently exhibited in the MRI scans. Therefore, we designed an optimal MRI sequence (3D GRE T2*) to enhance the visibility of gold markers. In this study, the designed sequence exhibited higher SNR, CNR and image quality, compared to CT. In addition, the size of the prostate in the MRI scan was found to be smaller compared to its size in the CT scans This finding has the potential to reduce the radiation exposure of healthy cells. The 3D GRE T2* sequence designed in this research has acceptable CNR, SNR and image quality. The SNR of prostate, fat, muscle and bone in GRE T2* images was higher than CT images, with a significant difference ($p < 0{\cdot}05$). Furthermore, the contrast of all tissues is more pronounced in GRE T2*, in comparison with CT, demonstrating statistically better results ($p < 0{\cdot}05$). Observations made by radiologists and oncologists indicate that the GRE sequence provides offers a more distinct display of gold markers, as opposed to CT.

Previous studies have stated that the differentiation of the gold indicators encounters difficulty within the T2 sequence.[7,11] Also it has been indicated that identifying gold markers in MRI is faced with significant challenges due to poor visualization of tissue edges and the presence of calcifications and vessels. Calcifications, which are observed in 40% of cases,[7] are frequently misidentified as gold markers, particularly in close proximity to the rectum. Through the research conducted by Soumya Ghose and colleagues, two sequences GRET1 and GRET2* were employed and GRE T1 sequence demonstrated the best display of gold markers.[7] However, that study was performed on a 3 Tesla scanner,[7] which made it impossible to apply the same GRE T1 sequence parameters on our 1·5 Tesla scanner because the lower strength of the magnetic field led to longer imaging times than patients could tolerate. Kapanen et al. utilized the GRE T2* sequence to visualize the gold marker in the prostate. This study highlighted the importance of phase cycling to reduce the banding artifact, enhance field uniformity and improve signal void of the gold marker.[11] Maria Schimidt et al. also used the GRET2* sequence to observe the gold marker.[4] Similarly, Schmidt et al. and Jonssone et al. identified GRET2* as the optimal sequence for gold markers in the intracranial targets, and we obtained analogous results using the same sequence in a different anatomical region which reinforces the versatility of the GRE T2* sequence and its reliable performance across various anatomical regions.[4,12]

In our study, 3D GRE T2* imaging revealed the volume of the prostate was 29·03% smaller than CT scan, which minimizes damage to healthy cells during radiotherapy. Similarly, Rasch et al. stated that the area of the prostate in CT is larger than in MRI, particularly around the seminal vesicle and apex regions. This observed disparity is more significant than it appears and bears noteworthy implications for radiotherapy treatment planning. MRI images, used for radiotherapy treatment planning, could lead to decreased radiation exposure to the urinary system and rectal diuresis areas.[13]

A study by Tanaka et al. was conducted in 2017 to design an MRI sequence for optimal imaging of the prostate and implanted markers for the radiotherapy treatment planning, for prostate cancer.[14] Their findings indicated that 2D and 3D GRE T2* sequences emerged as the most effective in concurrently visualizing both markers and prostate tissue.[14] The results of our investigation align with those reported in Tanaka's study, although there are some differences in methodological approaches. Methodological distinctions include the image assessment process. Tanaka's study involved three observers using a three-tiered classification, while our evaluation relied on two specialists in oncology and radiology, employing a five-level quality assessment. It should also be mentioned that our study implement a quantitative dimension by incorporating three criteria, including CNR, SNR and prostate volume, in addition to the qualitative criteria, enriching the comprehensive evaluation of imaging outcomes. Additionally, in Tanaka et al.'s study, the 3D GRE T2* sequence utilized time of repetition (TR)/TE1/deltaTE values of 37/14/7·3, respectively, on a 1·5T MRI scanner. In contrast, our study employed a 3D GRE T2* sequence with a TR of 70 milliseconds and TE of 18 milliseconds. The choice of a longer TR in our sequence is deliberate, as a longer TR allows for sufficient time for longitudinal magnetization

https://doi.org/10.1017/S1460396924000116 Published online by Cambridge University Press

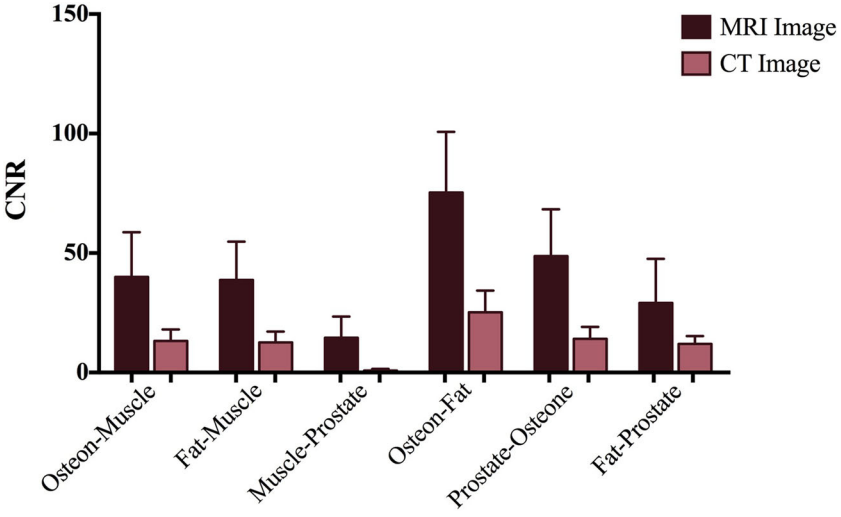

Figure 4. Comparison of different CNR (contrast to noise ratio) in CT scan (computed tomography) and MRI (magnetic resonance imaging) (3D GRE T2*).

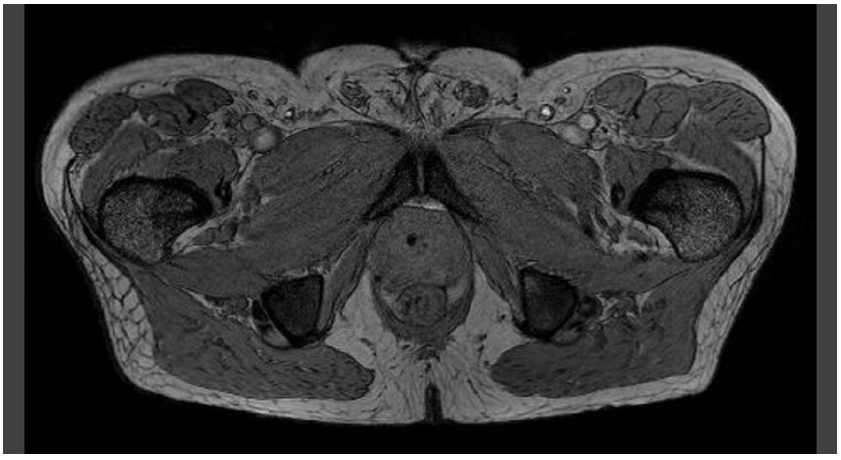

Figure 5. Image of optimized 3D GRE T2* of prostate and gold marker.

recovery, resulting in a higher SNR. Regarding TE, The extended TE in our sequence enhances the T2* effect, particularly beneficial for imaging metallic markers like gold.[15]

While our study provides insightful initial observations, a more robust foundation for the widespread adoption of the 3D GRE T2* sequence in contouring prostate and/or OARs for treatment planning necessitates comprehensive studies with increased participant diversity and statistical power. Such endeavors would contribute to affirming the generalizability and reliability of our current findings, guaranteeing the eventual translation of these observations into improved clinical practices for prostate cancer radiotherapy planning.

Conclusion

The comparison between the 3D GRE T2* sequence and the CT scan demonstrated that 3D GRE T2* was an excellent tool for displaying gold markers, The heightened visibility of gold markers facilitated by this sequence offers distinct advantages, enabling a more precise delineation of target areas and subsequently allowing for a more focused and refined radiation treatment planning. This potential to minimize collateral damage to healthy cells while enhancing the targeting precision on cancerous cells underscores the clinical significance of incorporating the 3D GRE T2* sequence in radiotherapy planning.

Data availability statement. The datasets from the current study are included within the article.

Acknowledgements. We acknowledge Dr. Hooman Dehkharghani for his consultation about the concept and design of the study.

Author contributions. FB: concept, design, data collection, data analysis, interpretation, writing the article, critical reviews, final approval. MB: data collection, data analysis, interpretation, writing the article, critical reviews, final approval. FF: concept, design, critical reviews, final approval. BB: writing the article, critical reviews, final approval. SA: data collection, critical reviews, final approval. FH: critical reviews, revision, final approval

Financial support. Not applicable.

Competing interests. The authors declare that the research was conducted in the absence of any commercial or financial relationships that could be construed as a potential conflict of interest.

Ethics approval. The Research Ethics Committees of Shahid Beheshti University of Medical Sciences approved the study proposal (4,124,554). The participants were informed about the aim of the study and were asked to sign the consent form. All data was kept confidential to preserve the identity of the participants.

Consent for publication. Not applicable

References

1. Sung H, Ferlay J, Siegel RL, et al. Global Cancer Statistics 2020: GLOBOCAN estimates of incidence and mortality worldwide for 36 cancers in 185 countries. CA Cancer J Clin 2021; 71 (3): 209–249.
2. Schieda N, Avruch L, Shabana WM, et al. Multi-echo gradient recalled echo imaging of the pelvis for improved depiction of brachytherapy seeds and fiducial markers facilitating radiotherapy planning and treatment of prostatic carcinoma. J Magn Reson Imaging 2015; 41 (3): 715–720.
3. Wu X, Gu J. Heritability of prostate cancer: a tale of rare variants and common single nucleotide polymorphisms. Ann Translational Med 2016; 4 (10): 206.
4. Schmidt MA, Payne GS. Radiotherapy planning using MRI. Phys Med Biol 2015; 60 (22): R323.
5. Huisman HJ, Fütterer JJ, van Lin EN, et al. Prostate cancer: precision of integrating functional MR imaging with radiation therapy treatment by using fiducial gold markers. Radiol 2005; 236 (1): 311–317.
6. Alzahrani M, Broadbent DA, Chuter R, et al. Audit feasibility for geometric distortion in magnetic resonance imaging for radiotherapy. Phys Imaging Radiat Oncol 2020; 15: 80–84.
7. Ghose S, Mitra J, Rivest-Hénault D, et al. MRI-alone radiation therapy planning for prostate cancer: automatic fiducial marker detection. Med Phys 2016; 43 (5): 2218–2228.
8. Gurney-Champion OJ, Lens E, van der Horst A, et al. Visibility and artifacts of gold fiducial markers used for image guided radiation therapy of pancreatic cancer on MRI. Med Phys 2015; 42 (5): 2638–2647.
9. Shinohara K, Roach M III. Technique for implantation of fiducial markers in the prostate. Urol 2008; 71 (2): 196–200.
10. Dawson LA, Litzenberg DW, Brock KK, et al. A comparison of ventilatory prostate movement in four treatment positions. Int J Radiat Oncol Biol Phys 2000; 48 (2): 319–323.
11. Kapanen M, Collan J, Beule A, et al. Commissioning of MRI-only based treatment planning procedure for external beam radiotherapy of prostate. Magn Reson Med 2013; 70 (1): 127–135.
12. Jonsson JH, Johansson A, Söderström K, et al. Treatment planning of intracranial targets on MRI derived substitute CT data. Radiother Oncol 2013; 108 (1): 118–122.
13. Rasch C, Barillot I, Remeijer P, et al. Definition of the prostate in CT and MRI: a multi-observer study. Int J Radiat Oncol Biol Phys 1999; 43 (1): 57–66.
14. Tanaka O, Komeda H, Hattori M, et al. Comparison of MRI sequences in ideal fiducial maker-based radiotherapy for prostate cancer. Rep Pract Oncol Radiother 2017; 22 (6): 502–506.
15. Hashemi RH, Bradley WG, Lisanti CJ. MRI: The basics: The Basics. Philadelphia, PA: Lippincott Williams & Wilkins; 2012.

https://doi.org/10.1017/S1460396924000116 Published online by Cambridge University Press